Theoretical Analysis of Quasi-Bessel Beam for Laser Micromachining

Wu Pinghui[1,2] Huang Wenhua[2]

([1] *State Key Laboratory of Modern Optical Instrumentation, Department of Optical Engineering, Zhejiang University, Hangzhou, Zhejiang* 310027, *China*
[2] *Department of Physics, Huzhou Teachers College, Huzhou, Zhejiang* 313000, *China*)

Abstract A quasi-Bessel beam can propagate over a long distance with its beam width unchanged, which provides a high beam aspect ratio, and is suitable for laser micromachining of structures. The propagation properties of quasi-Bessel beam generated by the ideal axicon and blunt-tip axicon are investigated. Strong peak oscillations occur due to interference between the quasi-Bessel beam and the refracted beam by the blunt-tip. Using the axicon for laser micromachining is theoretically calculated. Simple analytical formulas can be used to predict the required parameters, including laser pulse energy, generated fluence distribution, ablation width, beam aspect ratio and so on.

Key words laser optics; laser micromachining; axicon; quasi-Bessel beam
OCIS codes 140.3295; 140.3300; 140.3390

准贝塞尔光束在激光微加工中的理论分析

吴平辉[1,2] 黄文华[2]

([1]浙江大学光电系现代光学仪器国家重点实验室，浙江 杭州 310027
[2]湖州师范学院物理系，浙江 湖州 313000)

摘要 准贝塞尔光束具有能够远距离传输且保持光束宽度不变的特性，可以提供较大的光束纵横比，非常适合材料的激光微加工。研究了由理想轴棱锥和实际轴棱锥产生的准贝塞尔光束的传输特性。研究发现实际轴棱锥形成的准贝塞尔光束因干涉导致其轴上能量密度呈现强烈振荡的现象。重点分析了准贝塞尔光束在激光微加工中潜在的应用，通过推导获得的解析表达式可以用来预测激光加工所需的各项参数，包括激光脉冲能量、能量密度分布、消融宽度和光束纵横比等。

关键词 激光光学；激光微加工；轴棱锥；准贝塞尔光束
中图分类号 TN249 **文献标识码** A **doi**：10.3788/CJL201441.s102002

1 Introdution

Since laser micromachining using ultrashort pulses can generate highly reproducible micro- and nano-structures, they have been successfully applied to produce a wide range of structures such as waveguides, voids and channels. However, this technology still faces the challenge of producing high aspect ratio structures of submicron transverse dimensions because micromachining using focused traditional Gaussian beams suffers from the inevitable diffraction-induced tradeoff between beam waist and longitudinal interaction length. Recently, Bessel beams have attracted tremendous interest because of their unique properties, i. e., the ability to maintain narrow beam width over distances many times larger than the Rayleigh range and to self-heal behind obstacles or scatterers[1-3], which holds great promise for laser micromachining, other applications and the beam aspect ratio.

In this paper, we describe how to generate quasi-Bessel beam (QBB) using an axicon to improve the aspect ratio and allow the convenient micromachining of structures. Simple analytical formulas allow to predict the laser pulse energy, the generated fluence distribution and the ablation width.

2 Axicon-generated quasi-Bessel beam

An ideal Bessel beam exhibits an invariant intensity profile along the propagation direction and contains an

收稿日期：2013-10-20；**收到修改稿日期**：2013-11-08
基金项目：国家自然科学基金(11272120)
作者简介：吴平辉(1983—)，男，博士研究生，讲师，主要从事光电子技术方面的研究。E-mail：wph1021@163.com

infinite amount of energy, and hence is not possible to be generated experimentally. However, various approximate Bessel beams or quasi-Bessel beams have been demonstrated by annular aperture, axicon, Fabry-Perot etalon, computer-generated hologram or spatial light modulator[4-8]. It is generally preferred to use an axicon for laser machining due to its high efficiency. As shown in Fig. 1, a collimated Gaussian laser beam with the lateral intensity distribution $I(\rho)=I_0\exp(-2\rho^2/w^2)$ illuminates an ideal axicon of base angle α, where I_0 is the central intensity, w is the Gaussian beam waist. The propagation axis is the z-axis, with its origin at the axicon vertex.

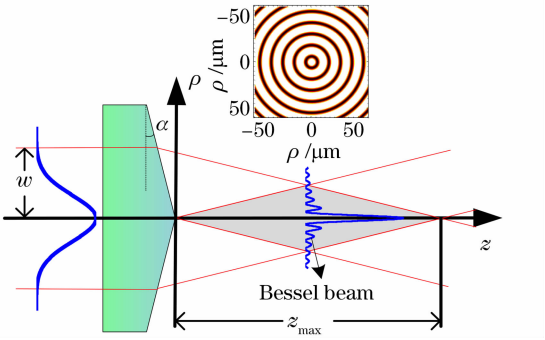

Fig. 1 Schematic of a QBB generated by an axicon. Inset is the cross-sectional profile of the QBB

For this case, the intensity distribution behind the axicon is described as[9]

$$I(\rho,w)=\frac{I_0\pi\beta w}{2}\left\{\left[F_1\left(\frac{\rho}{w}\right)+F_2\left(\frac{\rho}{w}\right)\right]^2 J_0^2(\rho\beta)+\left[F_1\left(\frac{\rho}{w}\right)-F_2\left(\frac{\rho}{w}\right)\right]^2 J_1^2(\rho\beta)\right\},\quad(1)$$

where ρ denotes radial coordinate, J_0 and J_1 are the zero-order and one-order Bessel function of the first kind, respectively, $\beta=k(n-1)\alpha=2\pi(n-1)\alpha/\lambda$, k is angular wavenumber, n is the refractive index of the axicon material, λ is the wavelength. The functions F_1 and F_2 are defined by

$$F_1\left(\frac{\rho}{w}\right)=\left(z_0+\frac{\rho}{w}\right)^{1/2}\exp\left[-\left(z_0+\frac{\rho}{w}\right)^2\right],\quad(2)$$

$$F_2\left(\frac{\rho}{w}\right)=\left(z_0-\frac{\rho}{w}\right)^{1/2}\exp\left[-\left(z_0-\frac{\rho}{w}\right)^2\right]\times H\left(z_0-\frac{\rho}{w}\right),\quad(3)$$

where $z_0=(n-1)\alpha z/w$, and H is the Heaviside step function

$$H=1\ \text{for}\ z_0\geqslant\rho/w,\quad(4)$$

$$H=0\ \text{for}\ z_0<\rho/w.\quad(5)$$

For small axicon base angle α, the axicon produces the QBB with depth of focus (DOF) z_{max} (Fig. 1), defined as

$$z_{max}=\frac{w}{(n-1)\alpha}.\quad(6)$$

An example of the optical intensity distribution generated by an ideal axicon as evaluated by Eq. (1) is shown in Fig. 2, which is calculated for $w=2$ mm, $\alpha=5°$, $n=1.5$ and $\lambda=1064$ nm. As can be observed, the QBB width remains a near constant with propagation distance, although the central intensity maximum varies axially. Besides, the DOF of this QBB is considerably longer than the DOF of that we have seen, for example, a Gaussian beam focused by a convex lens.

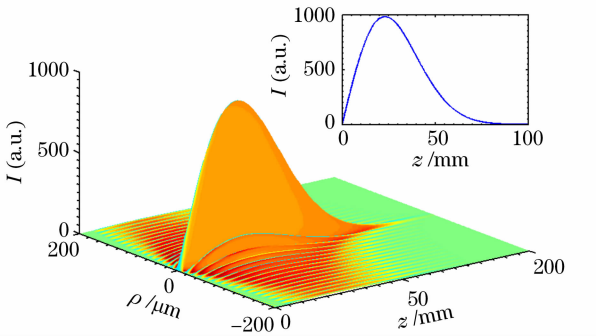

Fig. 2 Calculated intensity distribution behind an axicon illuminated by a Gaussian beam. Inset shows the axial intensity along the propagation direction

3 Theoretical calculation and results

For materials micromachining with ultra-short pulse lasers, the ablation is determined by the fluence F (laser energy per unit area) incident at the material surface. The intensity distribution of pulsed laser radiation depends on time. In most cases, the time dependence can be separated as $I(\rho,t)=I(\rho)f(t)$, and hence the fluence distribution can easily be calculated from the intensity distribution. Therefore the fluence is proportional to the time independent function $I(\rho)$ as

$$F(\rho)=\varepsilon I(\rho).\quad(7)$$

Integrate over ρ yields

$$2\pi\int_0^\infty\rho F(\rho)\,\mathrm{d}\rho=2\pi\varepsilon\int_0^\infty\rho I(\rho)\,\mathrm{d}\rho=Q,\quad(8)$$

where Q is the pulse energy. Because the laser power is equal to the incident power, the fluence distribution can be obtained by

$$F(\rho,w)=\frac{Q\beta}{w}\left\{\left[F_1\left(\frac{\rho}{w}\right)+F_2\left(\frac{\rho}{w}\right)\right]^2 J_0^2(\rho\beta)^2+\left[F_1\left(\frac{\rho}{w}\right)-F_2\left(\frac{\rho}{w}\right)\right]^2 J_1^2(\rho\beta)\right\}.\quad(9)$$

For reference, Fig. 3 shows the calculated fluence distributions for four typical wavelengths and two axicon base angles at the distance of $z_{max}/2$. The incident beam waist, pulse energy and refractive index are $w=2$ mm, $Q=100$ μJ and $n=1.5$, respectively. As can be observed, the fluence of central lobe is narrower for

shorter wavelength and larger axicon base angles.

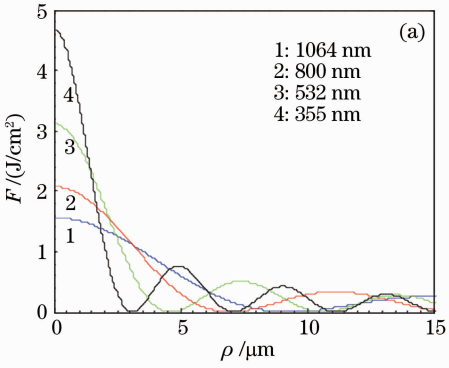

Fig. 3 Calculated fluence distributions for typical wavelengths for (a) $\alpha = 5°$ and (b) $\alpha = 10°$ at the distance of $z_{max}/2$

From Eq. (9), the peak fluence can be written as

$$F_{peak}(z) = \frac{4Q\beta z_0}{w}\exp(-2z_0^2). \tag{10}$$

Obviously, the maximum peak fluence $F_{peak}^{max} = \frac{2Q\beta}{w\sqrt{e}}$ occurs at

$$z = \frac{z_{max}}{2} = \frac{w}{2(n-1)\alpha}. \tag{11}$$

Another important parameter for laser micromachining is the ablation width, which can be estimated by the first root of the Bessel function J_0:

$$D \approx \frac{1.2\lambda}{\pi(n-1)\alpha}. \tag{12}$$

Figure 4 shows the expected ablation width as a function of axicon base angle for typical wavelengths. From Fig. 4 we find that the ablation widths present apparent downward trend with the increase of axicon base angle.

Based on the results described above, the QBB aspect ratio can be evaluated by $R = z_{max}/D \approx \pi w/(1.2\lambda)$. Fig. 5 shows the aspect ratio varies with incident beam waist for typical wavelengths. Remarkably, the aspect ratios can exceed 1000 or more, for example, a QBB at 1064 nm exhibits an aspect ratio as high as about 4900 for an incident beam with waist of 2 mm. Moreover, the value increases progressively along with the

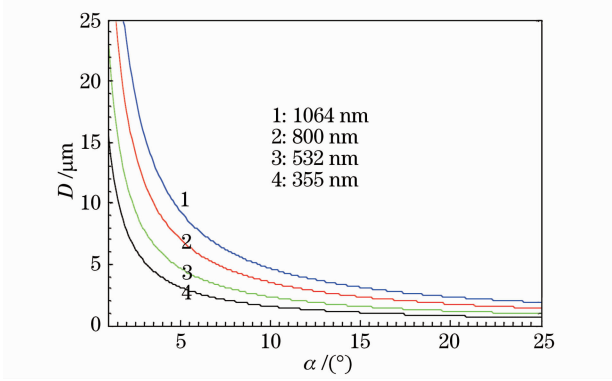

Fig. 4 Ablation width versus axicon base angle for typical wavelengths

increase of the incident beam waist. Such high beam aspect ratios are useful in the micromachining of high aspect ratio structures. For example, it is suitable for laser micromachining of deep nanochannel, which at present is a key technological issue in many important application fields. However, the existing technologies for material micromachining such as focused ion beam milling or deep reactive ion etching are not well suited to high aspect ratio micromachining.

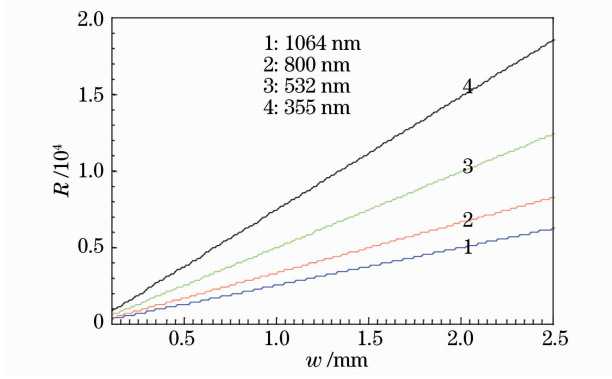

Fig. 5 Aspect ratio versus incident beam waist for typical wavelengths

As mentioned above, one of the attractive features of the QBB is its spatial invariance, i.e., the possibility of long-distance propagation without divergence, although the axial intensity varies smoothly along the beam propagation direction. This, however, is the case where we ignore diffraction effect on the axicon edges and assume a perfectly sharp axicon tip. In reality, an axicon suffers a number of imperfections, and the tip is rather blunt. Such imperfections cause strong axial oscillations that destroy the overall smooth profile of the propagating QBB. For laser micromachining of structures using a QBB, we should take into account the effect of blunt tip.

We calculate the electric field amplitude at the radial distance ρ and the distance z behind a blunt-tip axicon, by numerically solving the Fresnel Kirschoff integral [10]

$$E(\rho,z)=\frac{2\pi \mathrm{i}}{\lambda}\exp\left(-\frac{2\pi z \mathrm{i}}{\lambda}\right)\times$$
$$\int_0^{\infty}\frac{E(r_0,0)}{z}\exp\left[-\frac{(\rho^2+r_0^2)\pi \mathrm{i}}{\lambda z}\right]\mathrm{J}_0\left(\frac{2\pi\rho r_0}{\lambda z}\right)r_0\,\mathrm{d}r_0, \quad (13)$$

where $E(r_0,0)$ is the input electric field amplitude of Gaussian beam with waist w, and it can be written as

$$E(r_0,0)=E_0\exp\left[-\left(\frac{r_0}{w}\right)^2-\mathrm{i}\varphi(r_0)\right], \quad (14)$$

where $\varphi(r_0)$ is the spatial phase introduced by the axicon, and it is given by

$$\varphi(r_0)=\frac{2\pi(n-1)}{\lambda}d(r_0), \quad (15)$$

where $d(r_0)$ is the actual profile of the axicon. Akturk, Dépret, and Brzobohaty *et al.* have shown that the blunt-tip region of an axicon can be described by a hyperbola [10-12].

Assume that the profile of the axicon is a hyperboloid as described in Ref. [12]:

$$d(r_0)=\begin{cases}0.01-\sqrt{\dfrac{r_0^2}{125.7949}+0.0001} \\ \quad 0\leqslant r_0\leqslant 0.5\ \text{mm} \\ 0.01-\sqrt{\dfrac{r_0^2}{125.7949}} \\ \quad r_0>0.5\ \text{mm}\end{cases}. \quad (16)$$

According to Eq. (16), the profiles of axicons for blunt and ideal tips are shown in Fig. 6.

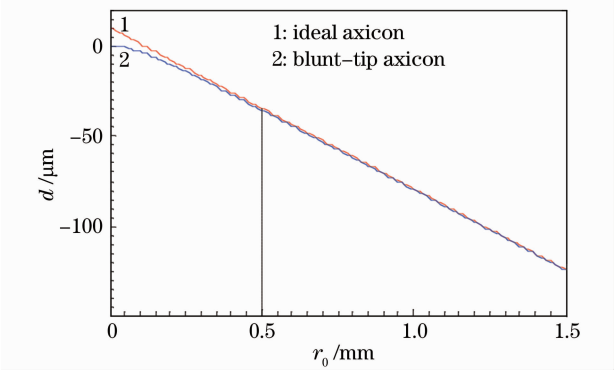

Fig. 6 Comparison of the blunt-tip axicon profile with the ideal axicon profile

In addition, the fluence distribution behind the axicon is investigated. Fig. 7 compares the peak fluences for the ideal axicon and blunt-tip axicon, here the calculated parameters are also in Ref. [12], i.e., $\alpha=5.095°$, $n=1.50699$ and $Q=1$ mJ, $\lambda=1064$ nm. Strong oscillating peak behavior for small distances from the axicon is clearly visible in Fig. 7. This is due to the interference between the QBB, formed by off-axis part of the axicon, and the wave refrected by the blunt-tip of the axicon. But for the longer distances, the peak fluence of blunt-tip axicon exhibits excellent coincidence with the ideal case. Such a fluence distribution can significantly influence laser micromachining results. We will introduce how to remove the undesired oscillations in other literatures.

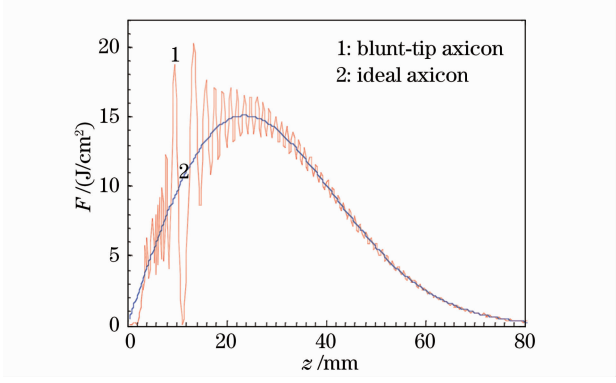

Fig. 7 Comparison of the peak fluence for the ideal axicon with the peak fluence for the blunt-tip axicon with input beam radius of 2.14 mm

4 Conclusion

A QBB possesses high beam aspect ratio, thus it is suitable for laser micromachining. The propagation properties of QQBs generated by the ideal axicon and blunt-tip axicon are analyzed. Significant peak fluence oscillations occur due to interference between the QBB and the refracted beam by the blunt-tip. Using the QQB for laser micromachining is theoretically calculated. Analytical formulas allow to predict the required laser parameters, including the laser pulse energy, the generated fluence distribution, the ablation width and the beam aspect ratio.

References

1 Courvoisier F, Lacourt P A, Jacquot M, *et al*.. Surface nanoprocessing with nondiffracting femtosecond Bessel beams [J]. Opt Lett, 2009, 34(20): 3163-3165.

2 Yu Y Y, Chang C K, Lai M W, *et al*.. Laser ablation of silicon using a Bessel-like beam generated by a subwavelength annular aperture structure[J]. Appl Opt, 2011, 50(34): 6384-6390.

3 Yalizay B, Ersoy T, Soylu B, *et al*.. Fabrication of nanometer-size structures in metal thin films using femtosecond laser Bessel beams[J]. Appl Phys Lett, 2012, 100(3): 031104.

4 Durnin J, Miceli J J Jr, Eberly J H. Experiments with nondiffracting needle beams[J]. J Opt Soc Am B, 1987, 4(13): 230.

5 Scott G, Mcardle N. Efficient generation of nearly diffraction-free beams using an axicon[J]. Opt Eng, 1992, 31(12): 2640-2643.

6 Cox A J, Dibble D C. Nondiffracting beam from a spatially filtered Fabry-Perot resonator[J]. J Opt Soc Am A, 1992, 9(2): 282-286.

7 Vasara A, Turunen J, Friberg A T. Realization of general nondiffracting beams with computer-generated holograms[J]. J Opt Soc Am A, 1989, 6(11): 1748-1754.

8 Davis J A, Guertin J, Cottrell D M. Diffraction-free beams generated with programmable spatial light modulators[J]. Appl

Opt, 1993, 32(31): 6368 - 6370.

9 Jarutis V, Paskauskas R, Stabinis A. Focusing of Laguerre-Gaussian beams by axicon[J]. Opt Commun, 2000, 184(1 - 4): 105 - 112.

10 Akturk S, Zhou B, Pasquiou B, *et al*.. Intensity distribution around the focal regions of real axicons[J]. Opt Commun, 2008, 281(17): 4240 - 4244.

11 Dépret B, Verkerk P, Hennequin D. Characterization and modelling of the hollow beam produced by a real conical lens[J]. Opt Commun, 2002, 211(1 - 6): 31 - 38.

12 Brzobohatý O, Čižmár T, Zemanek P. High quality quasi-Bessel beam generated by round-tip axicon[J]. Opt Express, 2008, 16(17): 12688 - 12700.

栏目编辑：史　敏